analytical chemistry

pubs.acs.org/ac Article

Development of a Highly Sensitive Enzyme-Linked Immunosorbent Assay for Mouse Soluble Epoxide Hydrolase Detection by Combining a Polyclonal Capture Antibody with a Nanobody Tracer

Dongyang Li, Yongliang Cui, Christophe Morisseau, Karen M. Wagner, Young Sik Cho, and Bruce D. Hammock*

Cite This: https://dx.doi.org/10.1021/acs.analchem.0c01511 Read Online

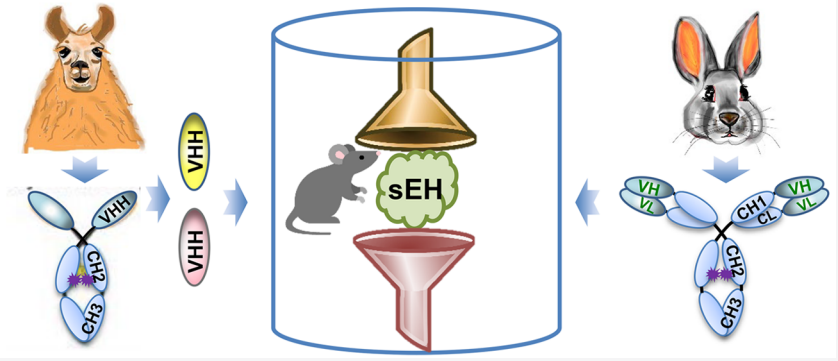

ABSTRACT: Enzyme-linked immunosorbent assays (ELISA) for the detection of soluble epoxide hydrolase (sEH), a key enzyme in the metabolism of fatty acids and a biomarker, may increasingly represent an important diagnostic tool. However, there is a lack of ELISAs for mouse sEH quantification, thus resulting in a bottleneck in understanding the pathogenesis of many diseases related to sEH based on mouse models. In this work, nanobodies recognizing mouse sEH were obtained through rebiopanning against mouse sEH in the previous phage display library of human sEH. Later, we developed four ELISAs involving a combination of anti-mouse sEH polyclonal antibodies (pAbs) and nanobodies. It was found that the double antibodies worked as dual filters and had a huge impact on both the sensitivity and selectivity of sandwich immunoassays. The switch from anti-human sEH pAbs to anti-mouse sEH pAbs led to over a 100-fold increase in the sensitivity and a dramatic decrease of the limit of detection to a picogram per milliliter range in format B (pAb/biotin-VHH/streptavidin-poly-horseradish peroxidase). Moreover, we found that the four sandwich ELISAs might demonstrate excellent selectivities to mouse sEH, despite the antibodies alone showing significant cross-reactivity to the matrix, indicating the enhanced selectivity of double antibodies as dual filters. Eventually, for the first time, the ELISA (format B) was successfully used to measure the mouse sEH level in cancer cells with ultralow abundances. The ELISAs proposed here represent a sensitive tool for tracking sEH in various biological processes and also provide deep insights into developing sandwich immunoassays against various targets in terms of both the sensitivity and selectivity.

Soluble epoxide hydrolase (sEH) is a 125 kDa dimer composed of two identical 62.5 kDa monomers and broadly distributed in multiple mammal tissues. It can metabolize many epoxy fatty acids (EpFAs) with potent anti-inflammatory properties, e.g., epoxyeicosatrienoic acids (EETs) and epoxydocosapentaenoic acids (EDPs), into their corresponding diols.[1] The inhibition of sEH can enhance the beneficial anti-inflammatory effects of EETs, and sEH therefore has become a potential pharmacological target for treating hypertension, vascular inflammation, cancer, pain, and multiple cardiovascular-related diseases involving inflammation.[1−4] A recent study by Ren et al.[5] reveals that sEH plays a key role in inflammation associated with the pathogenesis of Parkinson's disease (PD), further suggesting the feasibility of sEH as a biomarker for PD just as for other diseases.[6] Thus, the detection of sEH may represent an important diagnostic tool for health. The pathogenesis of many diseases related to sEH have been and continue to be studied based on mouse models. Currently, the most used methods for sEH detection include the activity-based radioactive (detectability of ∼50 ng/mL) or fluorometric (detectability of ∼10 ng/mL) assays and the

Received: April 8, 2020
Accepted: July 29, 2020

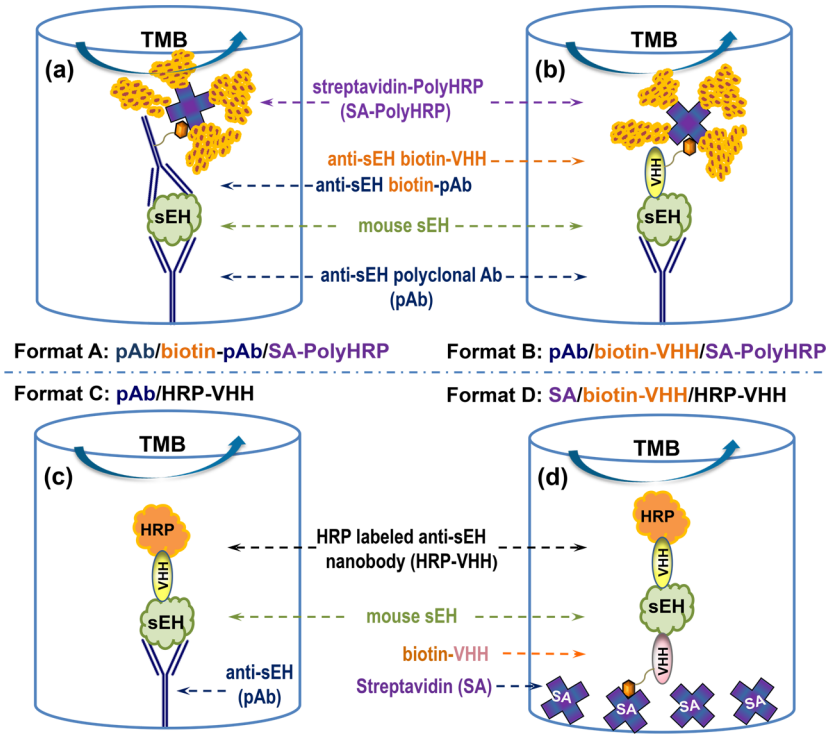

Figure 1. Schematic comparison of four different sandwich ELISA formats for mouse sEH detection: (a) format A (pAb/biotin-pAb/SA-Poly-horseradish peroxidase (SA-PolyHRP)), (b) format B (pAb/biotin-VHH/SA-PolyHRP), (c) format C (pAb/HRP-VHH), and (d) format D (SA/biotin-VHH/HRP-VHH). The switch of the detection antibody from biotin-pAb (format A) to biotin-VHH generates format B. The switch of the detection antibody plus tracer (formats A and B) to HRP-VHH results in format C. The switch of capture pAb (format C) to the streptavidin bridge plus biotin-VHH leads to format D.

antibody-based western blot (WB, detectability of ~1 ng) assay.[7,8] However, the radioactive assay has drawbacks due to radiation-associated health and safety concerns for personnel, high cost, and commercial unavailability of substrates. The fluorometric assay has a high background from substrate hydrolysis and is not applicable to tissue extracts.[8] The WB assay is semiquantitative, time-consuming, and only moderately insensitive. It also has the limitations of high technical demand and large interoperator variability.[9] Thus, excellent detection methods for mouse sEH, other than activity-based assays and WBs, are needed.

The enzyme-linked immunosorbent assay (ELISA) has been widely employed to detect numerous analytes due to its overwhelming advantages in sensitivity, speed, simplicity, cost, throughput, and safety.[10−15] It is also promising for the analysis of mouse sEH. The essential key for a good ELISA is the availability of good antibodies, which majorly determine the sensitivity and specificity of the assay. A nanobody (also termed VHH) is a single domain antibody recombinantly derived from heavy-chain-only antibodies in camelids or cartilaginous fish.[16,17] It is increasingly attractive and has been used in various immunoassays due to its small size (~15 kDa), monoclonal nature, thermostability, genetic manipulability, and capacity for continuous manufacturing.[18−23] In our previous work, we developed nanobody-based immunoassays for the detection of human sEH.[18,24] However, these immunoassays were highly selective for human sEH and did not effectively recognize the sEH from other species. The development of ELISAs against mouse sEH was therefore pursued, given the central role of murine models in *in vivo* experiments.

The initial purpose of this study was to obtain nanobodies recognizing the mouse sEH through rebiopanning the existing phage display library of human sEH against the new analyte and then to develop immunoassays based on these nanobodies. However, the switch of the capture antibody resulting in an unexpected dramatic increase of the sensitivity and the sandwich ELISAs demonstrating no recognition to potential interferences, which the antibodies alone showed significant cross-reactivity to, highlighted the dual filter effect of double antibodies. Although the sandwich immunoassay was first developed decades ago in 1973[25] and its advantage in sensitivity over a competitive immunoassay is well recognized, its theoretical enhanced selectivity was rarely confirmed with exact experimental data. Using the mouse sEH as the model analyte, we developed four formats of sandwich ELISAs involving double antibodies in combination of pAb/pAb (format A), pAb/nanobody (formats B and C), and nanobody/nanobody (format D), as illustrated in Figure 1. The dual filter effect of the double antibodies were highlighted in terms of the sensitivity and selectivity of these four ELISAs. The validation completed on the matrix effect and analysis of mouse cancer cells further indicated the success of the immunoassays.

EXPERIMENTAL SECTION

Materials. Recombinant mouse sEH, protein A column affinity purified rabbit anti-mouse sEH, and anti-human sEH pAbs were produced by our laboratory as described elsewhere.[24,26,27] Sodium periodate, horseradish peroxidase (HRP), streptavidin, bovine serum albumin (BSA), and sulfo-*N*-hydroxysuccinimide (NHS)-LC-biotin were bought

https://dx.doi.org/10.1021/acs.analchem.0c01511
Anal. Chem. XXXX, XXX, XXX−XXX

from Sigma-Aldrich. High-binding microplates (Nunc Maxisorp, cat. no. 442404) were purchased from Thermo Fisher Scientific Inc. Streptavidin-PolyHRP40 conjugates (SA-PolyHRP) were purchased from Fitzgerald Industries International (Concord, MA).

Rebiopanning of Phage Anti-Mouse sEH VHH Clones. The existing phage display library of human sEH was rebiopanned against the mouse sEH following our previous work[24] but using the sEH from mice instead of humans. Briefly, mouse sEH was first biotinylated and then bound to streptavidin-coated magnetic beads (Pierce). The resultant beads were prewashed (10 μL, 16 μM), and the phage VHH library (100 μL, 10^{13} plaque-forming units (PFU)/mL) were added to the same microwell preblocked with 0.01 M phosphate buffer (pH 7.4) containing 2% BSA (PBB). After incubation, the beads were washed five times with PBB (300 μL). Then, the bound phages were eluted through the addition of glycine-HCl buffer (pH 2.2). The eluted phages were reamplifed and used again on the next round of panning. After four rounds of panning in the same manner but with gradually decreased concentrations of mouse sEH (16, 16, 8, and 4 μM), positive clones were identified through the phage ELISA and then sequenced. Nine anti-mouse sEH VHH phage clones (3A2, 3C1, 3C5, 3C9, 4C3, 4C7, 4C10, 4C11, and 4C14) with different amino acid sequences were obtained, as illustrated in Figure S1. The corresponding nanobodies were later expressed in *Escherichia coli* and purified against their 6xHis-tag.

Biotinylation of Antibodies and Preparation of HRP-Nanobody Conjugates (HRP-4C3). Antibodies were biotinylated through amine coupling according to our previous work.[18] Briefly, fresh sulfo-NHS-LC-biotin (10 mg/mL in PBS of pH 7.4) was rapidly added to anti-mouse sEH pAb and nanobodies at a molar ratio of 20:1 and 10:1, respectively. After 1 h of reaction at room temperature (RT) with gentle shaking, free biotin was removed through extensive dialysis (molecular weight cut-off (MWCO) of 3000) at 4 °C. The resultant biotinylated antibodies were stored in aliquots at −20 °C until use.

HRP-labeled nanobodies were prepared through periodate oxidation but in mild conditions (pH 5.4, 10 mM $NaIO_4$, 30 min, ice bath) with high working concentrations of HRP according to ref 28. Briefly, 10 μL of 260 mM stocking $NaIO_4$ was premixed with 130 μL of 0.2 M acetate buffer (pH 5.4). Then, 70 μL of the resultant mixture was added to 60 μL of 20 mg/mL HRP in Milli-Q water, followed by the immediate color change of HRP from brownish to green due to $NaIO_4$ oxidation. The oxidation was allowed to proceed for 30 min on an ice bath in the dark with shaking (100 rpm) and then quenched through a Zeba spin desalting column (MWCO of 7000). Nanobodies were then added to the periodate-oxidized HRP at a molar ratio of 1:1, with the pH adjusted to an alkaline range using sodium carbonate buffer (pH 9.5). After 2 h of coupling in the dark at RT with shaking (600 rpm), the unstable Schiff base formed was further reduced to a secondary amine with sodium cyanoborohydride (*caution*: cyanoborohydride is very toxic and should be used in a fume hood). The unreacted aldehyde sites were then blocked with glycine. The resultant conjugate mixture was further separated with fast protein liquid chromatography (FPLC) with Next Generation Chromatography system plus Enrich size exclusion chromatography 650 (10/300 mm) column from Bio-Rad. The fractions before the HRP fraction peak were collected, concentrated, and stored in 50% glycerol/PBS at −20 °C until use. The HRP-labeled nanobody conjugate (HRP-VHH) obtained in this way is free of unbound HRP and unbound nanobodies. It may produce high signal-to-noise ratio as a detection antibody.

Test of Nanobody Performance Using Different pAbs as the Capture Antibodies in Format B. Anti-human sEH pAb or anti-mouse sEH pAb was coated at 2.5 μg/mL in 0.05 M (pH 9.6) carbonate-bicarbonate buffer (CB) overnight at 4 °C on a high-binding Nunc microplate (100 μL/well). After washing, 250 μL of 3% (w/v) skim milk/PBS was used to block each well for 1 h. After another washing, serial concentrations of mouse sEH calibrators in the standard diluent (PBS containing 0.1 mg/mL BSA) were then added to the plate (100 μL/well), followed by the immediate addition of biotinylated nanobodies (biotin-VHHs, 1 μg/mL, 100 μL/well) in PBS. The immunoreaction was allowed to last for 1 h. After washing, the tracer SA-PolyHRP was added (25 ng/mL, 100 μL/well) and incubated for 30 min. After the final washing, color development using 3,3′,5,5′-tetramethylbenzidine (TMB) substrate (100 μL/well, recipe from ref 28) was allowed to proceed for 15 min. The optical density (OD) was measured at 450 nm within 10 min after terminating the color development with 1 M sulfuric acid (100 μL/well). Unless otherwise stated, all incubations were conducted at room temperature with shaking (600 rpm) on a microplate shaker, and each washing step included three washings with PBS containing 0.05% Tween-20 (PBST, 300 μL/well) using a plate washer.

Construction of Calibration Curves for Mouse sEH detection in Four ELISA Formats. As shown in Figure 1, four formats of sandwich ELISAs involving double antibodies in combinations of pAb/pAb, pAb/nanobody, and nanobody/nanobody were performed. The three formats (A, C, and D) were run similarly to format B, as aforementioned, but with one or two steps different in each run. For format A, biotinylated anti-mouse sEH pAb (biotin-pAb, 0.25 μg/mL) was used as the detection antibody. For formats C and D, HRP-labeled nanobodies (HRP-4C3, 0.72 mg/mL) at 1:4000 dilution were used as the detection antibodies, with no need for secondary tracers. However, format D adopted nanobodies (3C1) instead of pAb as the capture antibodies. This nanobody was first biotinylated and then immobilized on the polystyrene surface via a streptavidin bridge for good capture performance according to our previous finding.[18] The selection of the nanobody pair is detailed in Figure S4. The same reagents involved in these four formats were used from the same batch.

pAb-Based Western Blot and Selectivity Test for Sandwich ELISAs. The selectivity of anti-mouse sEH pAb was characterized using a WB assay against the liver tissues from sEH knock-out (KO) and wild-type (WT) mice. Brifely, proteins in the homogenates were separated through sodium dodecyl sulfate−polyacrylamide gel electrophoresis (SDS-PAGE) and transferred to a nitrocellulose membrane via a trans-blot turbo transfer system (Bio-Rad). The membrane was blocked with TBS containing 5% skim milk and 0.1% Tween-20 for 1 h at RT. After washing, anti-mouse sEH anti-serum (1:5000) was added and incubated overnight at 4 °C. Then, the membrane was washed and later incubated with HRP-anti-rabbit IgG from Cell Signaling Technology at a 1:10000 dilution in TBS containing 5% skim milk and 0.1% Tween-20 for 1 h at RT. After washing, the membrane was incubated with the clarity western enhanced chemiluminescence substrate (Bio-Rad) and visualized using the ChemiDoc gel

https://dx.doi.org/10.1021/acs.analchem.0c01511
Anal. Chem. XXXX, XXX, XXX−XXX

image system from Bio-Rad. In addition, the selectivity of the four sandwich ELISAs were verified against eight tissues from sEH KO and WT mice, including scapular brown adipose tissue (BAT), epididymal white adipose tissue (WAT_Ep), inguinal white adipose tissue (WAT_Ig), liver, kidney, brain, heart, and mesenchymal fat pad (MFP). All KO and WT tissues are taken from one KO mouse and one WT mouse, respectively; both mice are age matched and housed under the same conditions for the duration of the experiment. Briefly, these tissues were flash-frozen post-necropsy and stored at −80 °C until the assay. For the assay, the tissues were weighed and homogenized in PBS buffer containing a protease inhibitor, and the protein was quantified by a bicinchoninic acid assay. The samples were then diluted 100-, 1000-, 10000-, and 100000-fold on the deep-well plate and added to the ELISA plates with a multichannel pipet. The other steps were the same as that in the four ELISAs above-described.

Matrix Effects. Nanobody-based ELISAs (formats C and D) representing the pAb/nanobody and double nanobodies were chosen for the evaluation of the matrix effect. Hepatic cytosol samples from KO mice were tested based on a simple dilution protocol. Briefly, the hepatic cytosol samples were diluted with standard diluent to 1:100, 1:1000, and 1:10000. Afterwards, series of mouse sEHs were spiked into the assay buffer of the standard diluent and the diluted matrixes. The resultant calibrators on different matrixes were run in the ELISA of formats C and D.

Analysis of Cancer Cells *In Vitro* with Ultralow Expression of sEH. Eight different cancer cells were cultivated *in vitro* (~10^5 cells/mL), including Lewis lung cancer, T241 fibrosarcoma, B16F10 melanoma, 4T1 breast adenocarcinoma, E0771 breast adenocarcinoma, MC38 colon adenocarcinoma, CT26 colon adenocarcinoma, and ID8 ovarian adenocarcinoma. Eight samples of each kind from the first batch (sample nos. 1−8) and four samples of E0771/CT26 from the second batch (sample nos. 9−12) were simultaneously analyzed using formats C and B with a higher sensitivity. Dilutions generating signals in the linear section of the calibration curves were employed to calculate the mouse sEH level in the samples.

RESULTS AND DISCUSSION

Performance Difference of Capture pAbs against Mouse sEH. Nine different nanobodies (3A2, 3C1, 3C5, 3C9, 4C3, 4C7, 4C10, 4C11, and 4C14) recognizing mouse sEH were obtained, and their amino acid sequences are listed in Figure S1. The preliminary test was conducted in ELISA (format B) using those biotinylated nanobodies (1 μg/mL) as detection antibodies, rabbit anti-human sEH pAb (2.5 μg/mL) as capture antibodies, and a potent PolyHRP-based tracer (SA-PolyHRP, 25 ng/mL) as the tracer. As shown in Figure 2a, the nine nanobody-based ELISA demonstrated a sufficient OD in the range from 0 to 250 ng/mL of mouse sEH. This is, however, one order weaker than previous developed PolyHRP ELISA for human sEH.[18] This gave us an early impression that the affinities of nine nanobodies against mouse sEH were likely poorer than that of the previous nanobodies against human sEH, considering the phage display library used was the one constructed using llama blood with human sEH immunized. To our surprise, the switch of capture Ab from anti-human sEH to anti-mouse sEH pAb (2.5 μg/mL) led to approximately 100-fold stronger signal responses (see Figure 2b and Table S1). This dramatic enhancement of the sensitivity can be

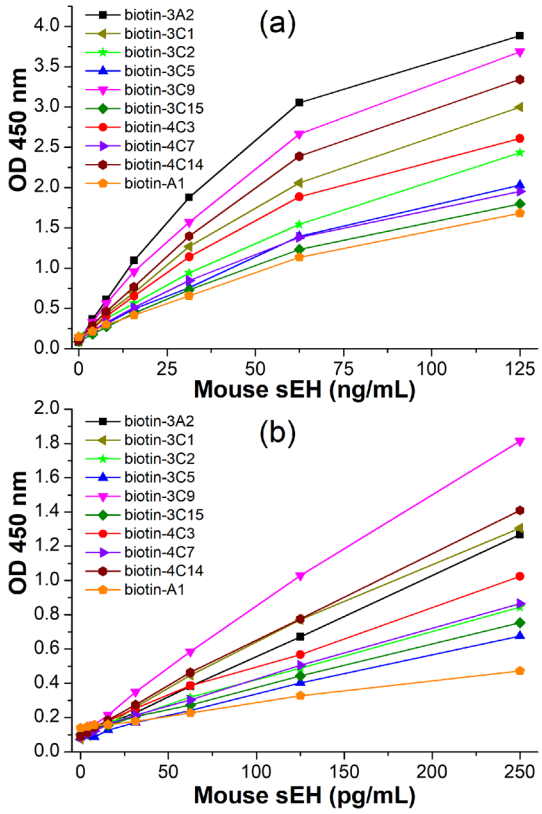

Figure 2. Signal responses of nine rebiopanned nanobodies, with A1 as a detection antibody (1 μg/mL) after biotinylation and SA-PolyHRP (25 ng/mL) as the tracer for mouse sEH detection in format B using different affinity-purified pAb (2.5 μg/mL) as capture antibodies: (a) rabbit anti-human sEH pAb and (b) anti-mouse sEH pAb. The inclusion of A1 will be discussed with Figure 4.

attributed to the increased affinity and avidity of polyclonal Ab obtained through immunization with mouse sEH instead of human sEH. This pAb possessed more produced antibody clones that recognized various epitopes of mouse sEH and a higher affinity to mouse sEH than human sEH by chance in that immunization. The surprising supersensitivity of ELISA in Figure 2b removed our initial illusion of the nine nanobodies against mouse sEH and further confirmed the importance of efficient capture antibodies. However, the anti-mouse sEH pAb still has the issues of limited supply and potential high cross-reactivity to interferences. Considering the excellent capture capability of the anti-mouse sEH pAb, the monoclonal nature and continuous supply of the nanobodies, and the difference of the tracer, hereby we developed four different ELISAs, as illustrated in Figure 1, to compare and provide a comprehensive guideline for mouse sEH sandwich ELISA.

Comparison of Calibration Curves of Four Sandwich ELISA Formats. Comparing pAbs and nanobodies is a compelling topic. However, it is hard to compare these two classes of antibodies, since the immune responses can vary significantly, even in genetically identical immunized animals. In addition to this, the chosen clones might show a large difference in affinities, depending on the employed screening techniques and the random effects in the panning of nanobodies. Thus, it is difficult to draw conclusions for an overall comparison of these two classes of antibodies based on limited quantities of antibodies used. However, the comparison of sandwich ELISAs involving pAbs and nanobodies may still

https://dx.doi.org/10.1021/acs.analchem.0c01511
Anal. Chem. XXXX, XXX, XXX−XXX

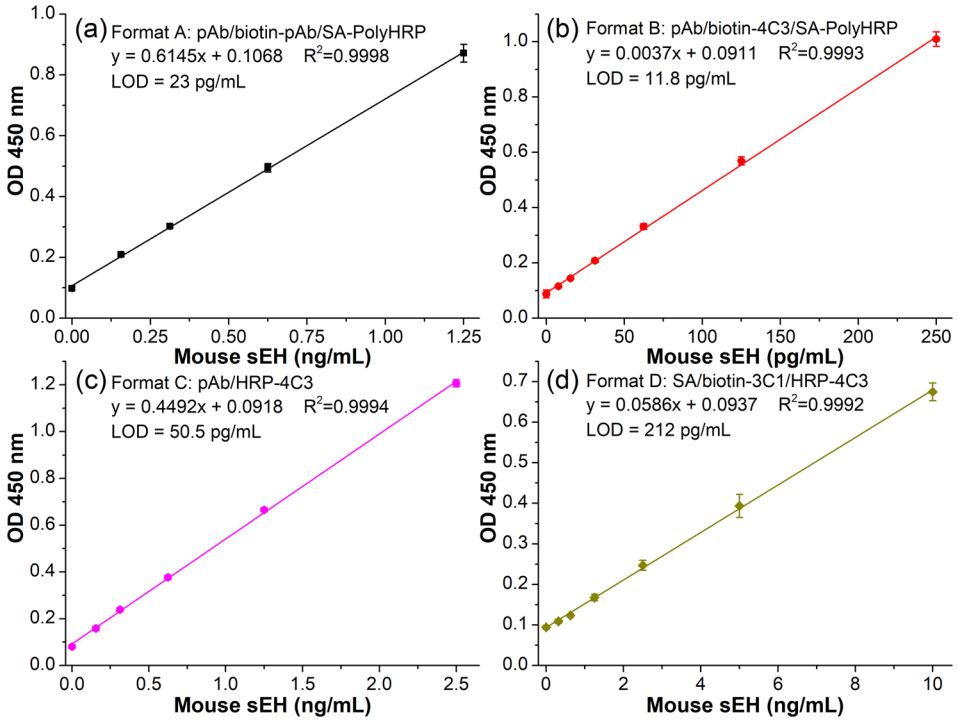

Figure 3. Calibration curves of four sandwich ELISA formats for mouse sEH detection: (a) format A, coating anti-mouse sEH pAb (2.5 μg/mL, 18 h), 3% SM blocking (1 h), biotin-pAb (0.25 μg/mL, 1 h), and SA-PolyHRP (25 ng/mL, 0.5 h); (b) format B, coating anti-mouse sEH pAb (2.5 μg/mL, 18 h), 3% SM blocking (1 h), biotin-4C3 (1 μg/mL, 1 h), and SA-PolyHRP (25 ng/mL, 0.5 h); (c) format C, coating anti-mouse sEH pAb (2.5 μg/mL, 18 h), 3% SM blocking (1 h), and HRP-4C3 (1:4000, 1 h); (d) format D, coating streptavidin (2.5 μg/mL, 18 h), 2% BSA blocking (1 h), biotin-3C1 (1.25 μg/mL, 1 h), and HRP-4C3 (1:4000, 1 h). TMB color development is 15 min for each format before stopping with 1 M H_2SO_4. Error bars indicate standard deviations (n = 3).

provide a reference for understanding these two classes of antibodies in immunoassay development. We tested four formats of sandwich ELISA for mouse sEH detection, as illustrated in Figure 1. Each format has its feature and may vary in performance. Formats A and B belong to the indirect sandwich ELISA, which involves a step for adding a tracer after the detection antibodies, while formats C and D belong to the direct sandwich ELISA, with no need for an extra tracer due to the enzyme-labeled detection antibody used. The latter saves one step in terms of reagent cost, labor, and time. Regarding the comparison of different assays, both the limit of detection (LOD) and sensitivity are informative parameters, but we believe the sensitivity (slope) is a much more robust index than the LOD, as deeply discussed in our previous work.[18,28] For formats A−C, the optimal working concentration of capture pAbs was found to be 2.5 μg/mL (data not shown), which is used throughout this work. Format A employed biotinylated pAbs as the detection antibodies and SA-PolyHRP as the tracer. Its calibration curve demonstrated a sensitivity of 0.6145 OD·mL/ng and a LOD of 23 pg/mL, as shown in Figure 3a. Herein, sensitivity refers to the slope, and the LOD is the calculated concentration corresponding to the signal response of the blank plus three times its standard deviation. The replacement of biotinylated pAbs with biotinylated nanobodies (biotin-4C3) leads to format B. Its calibration curve, shown in Figure 3b, gave a sensitivity of 3.7 OD·mL/ng and a LOD of 11.8 pg/mL. This sensitivity is 6-fold greater than that of format A. The enhancement can be attributed to the high working concentration (1 μg/mL) and thereby the high molar quantities of biotin-4C3. This is allowed by the low nonspecific background likely resulting from the feature of VHH in an excellent solubility and lack of an Fc region, whereas the Fc-containing IgG normally only allows working concentrations of sub-microgram per milliliter for detection antibodies due to the relatively severe nonspecific adsorption. The switch of detection antibodies plus tracers (formats A and B) to HRP-labeled nanobodies leads to format C. HRP-labeled nanobodies (HRP-4C3) prepared in this work possessed an average of 3.1 nanobodies per HRP, as calculated from its adsorption at 280 and 403 nm. As shown in Figure 3c, format C generated a sensitivity of 0.4492 OD·mL/ng and a LOD of 50.5 pg/mL when the working concentration of HPR-4C3 was used in a 1:4000 ratio. This sensitivity is still very high in immunoassays; however, it is almost 1 order of magnitude lower than that of format B. Moreover, format C saved the secondary tracer step and the reagent cost, labor, and time involved. However, formats A−C employed the pAbs as capture antibodies and thus might suffer from the limited supply of pAbs. The switch of capture pAbs (format C) to streptavidin bridge plus biotin-VHH leads to format D. This streptavidin-bridged double nanobody ELISA is chosen according to our recent work,[18] which demonstrated this format was much more sensitive than the double nanobody ELISA with capture nanobodies passively adsorbed. As shown in Figure 3d, format D demonstrated a sensitivity of 0.0586 OD·mL/ng and a LOD of 212 pg/mL for mouse sEH detection. This sensitivity is merely 13% of format C using the same detection antibodies. It again indicated the ultrahigh affinity or avidity of the anti-mouse sEH pAb used, for the previous capture anti-human sEH pAbs described in ref 28 in similar comparisons for human sEH detection gave a 3.1-fold greater performance of streptavidin-bridged capture nano-

https://dx.doi.org/10.1021/acs.analchem.0c01511
Anal. Chem. XXXX, XXX, XXX−XXX

bodies. From these comparisons, we can understand how the capability of the capture antibody can make huge differences in the sensitivity of the sandwich immunoassay. The capture antibodies worked as a filter and could retain the analyte to some extent for further formation of the sandwich immunocomplex, depending on its affinity. Also, the detection antibodies and the tracers can influence the overall sensitivity of the immunoassay. The four formats in this work provided a portfolio of an immunoassay with different sensitivities and antibody types.

Antibody Recognition versus Immunoassay Selectivity. A good immunoassay should be able to distinguish the analyte from interferences, thus avoiding false positive results. Generally, the recognition capability or selectivity of sandwich immunoassays is evaluated by the selectivity coefficient, a measure of its sensitivity for an interfering agent relative to that for the analyte. However, it is important to differentiate the recognition capability of an antibody from that of an immunoassay. The recognition capability of an antibody can be measured with its specificity and selectivity, defined by the number and the uniqueness of the epitope to which the antibody binds, respectively.[29] When the specificity is low, the antibody will recognize several different epitopes. The highest specificity is achieved when the antibody binds to only one epitope. Thus, monoclonal antibodies and nanobodies are inherently specific, and polyclonal antibodies are inherently less specific.[29] However, there is no absolute correlation between the specificity and selectivity. When the antibody selectivity is low, the epitope is shared with other interferences. The selectivity increases when the epitope is unique for the analyte, while other interferences that are present will not be detected. As illustrated in Figure 4a, the anti-mouse sEH

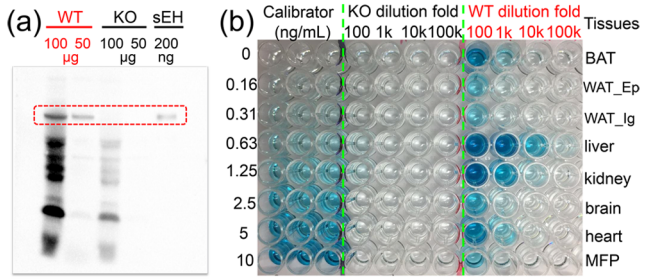

Figure 4. Antibody recognition versus immunoassay selectivity. (a) The selectivity of anti-mouse sEH pAb against hepatic cytosol samples of sEH knockout and wild-type mice through western blot analyses. (b) The selectivity of double pAb-based ELISA (format A) against eight kinds of tissues from sEH KO and WT mice.

polyclonal anti-serum showed cross-reactivity to several nontarget protein bands in the denatured SDS-PAGE-based western blot for liver tissues of both sEH KO and WT mice. This indicates the existence of a shared epitope between sEH and other proteins in the matrix and thus the poor selectivity of this polyclonal antibody. The selectivities of the nine nanobodies were not determined by the western blot analysis since the nanobodies did not recognize the denatured antigen.

In the literature, the measurement of the immunoassay selectivity was always done by comparing the analyte with a group of analogues, some of which are even not included in the matrix of the real samples. An inherent limitation in this strategy is that the quality of the selectivity may vary with the numbers of available potential interferences. Moreover, many unknown components in the real matrix cannot be evaluated. Thus, for the evaluation of the analyte of a protein, it is best to test the analyte-knockout matrix. In this work, eight tissues from a sEH KO mouse were collected and tested in sandwich ELISAs; also, the corresponding tissues from WT mice were tested simultaneously as the positive controls. Interestingly, as shown in Figure 4b, the double pAb-based ELISA (format A) did not generate signal responses to the KO tissues, while it demonstrated strong signal responses to the WT tissues. This indicates that format A recognizes nothing but sEH in these mouse tissues, thus indicating the excellent selectivity of the assay. The only explanation for the high selectivity of this ELISA based on the poor selectivity of the pAb is that there was just one shared epitope between sEH and other interfering proteins in the matrix. When the interfering proteins were captured by the first antibody, they could not be bound to the second antibody for the formation of the sandwich immunocomplex. This increased selectivity highlights the dual filter effect of the double antibodies in the sandwich ELISA. On the other hand, the single antibody-based immunological techniques have higher odds of producing false-positive results, especially when no extra control is involved, e.g., immunohistochemistry (IHC). Hudson et al. once reported that the HIV regulatory protein Tat was not detected by sandwich ELISA but could be detected immunohistochemically in protein extracts from the brains of the same groups of patients.[30] This unexplained difference in analyte recognition can be well explained now by the aforementioned better selectivity resulting from the double antibodies in the sandwich ELISA. In addition to format A, the ELISAs in formats B, C, and D similarly demonstrated robust signal responses in WT tissues and no signal responses in KO tissues (see Figure S2). Thus, we can conclude that all four formats of the sandwich ELISA demonstrated good selectivity for mouse sEH in real samples. In addition, from Table 1, we can see that the relative sEH abundance among the eight WT tissues were similar in each format. However, higher values in WT tissues were obtained generally for the ELISA format with higher sensitivities. This is because the higher sensitivity allows more working dilutions of the samples and thus lower matrix effects.

To further determine the selectivity of the nine nanobodies, both sEH KO and WT mice tissues at varying dilutions were coated on the high-binding microplate and detected with the nanobodies. The anti-mouse sEH pAbs were also used as detection antibodies for comparison. The results are shown in Figure S3. As expected, the anti-mouse sEH pAb showed strong recognition to both the KO and WT tissues, further confirming its cross-reactivity to the undenatured matrix. However, the nine nanobodies unexpectedly also showed strong signal responses to both the KO and WT tissues. The strongest possible explanation for the cross-reactivity of the monospecific nanobody to the KO matrix is that all these nine nanobodies recognized the same epitope shared by sEH and the interfering proteins in the matrix. To further validate this hypothesis, epitope mapping of the nanobodies was performed based on the completion assay (see Figure S4a). As shown in Figure S4b, the nine nanobodies showed inhibition to each other, indicating these nanobodies recognize the same epitope. Despite recognition of the same epitope, these nanobodies with different sequences of amino acids may have different physicochemical properties. For example, we observed the inactivation of the clone 3A1 but good functionality of 4C3

https://dx.doi.org/10.1021/acs.analchem.0c01511
Anal. Chem. XXXX, XXX, XXX−XXX

Table 1. Selectivity Tests of Four ELISA Formats (A, B, C, and D) against Tissues from WT Mice[a]

		mouse sEH (ng/mL) in neat samples				working dilutions used in ELISAs			
WT tissues[b]	sEH activity[c]	A	B	C	D	A	B	C	D
BAT	54.9	828	993	743	384	1k	10k	1k	100
WAT_Ep	4.4	189	194	130	n.d.	1k	1k	100	100
WAT_Ig	6.6	130	167	120	n.d.	100	1k	100	100
liver	976.8	29801	37866	31691	24990	100k	1000k	100k	10k
kidney	186.7	4905	6759	5438	3181	10k	100k	10k	1k
brain	13.8	301	369	294	n.d.	1k	10k	1k	100
heart	85.4	1199	1842	1399	1009	1k	10k	1k	100
MFP	28.9	208	282	217	67	1k	1k	100	100

[a]n.d. = not determined (below LOD); 1k = 1000. [b]tissues: scapular brown adipose tissue (BAT), epididymal white adipose tissue (WAT_Ep), inguinal white adipose tissue (WAT_Ig), mesenchymal fat pad (MFP). [c]The activity (nmol/(min·mL)) was measured with radioactive assays using [^{3}H]-trans-1,3-diphenylpropene oxide (*t*-DPPO) as the substrate. No appreciable activity was found in eight corresponding KO tissues, with background values of 0.05 nmol/(min·mL).

after conjugation to the same periodate-oxidized HRP (data not shown). In addition, the feasibility of the double nanobody ELISA (format D, 3C1/4C3) can be attributed to the dimer structure of mouse sEH, which possessed two identical epitopes. In addition, the clone 4C3 and the previous nine anti-human sEH nanobodies in ref 18 were put together for epitope mapping. The results indicated that the 4C3 recognized the same epitope as the group of clones A1, B4, and B7 did. The recognition to the mouse sEH of A1 in previous works was not known because it resulted from the use of anti-human sEH anti-serum as the capture antibody in selectivity tests. The simultaneous comparison with the eight rebiopanned nanobodies shown in Figure 2 confirmed the recognition capability of A1 to mouse sEH. Also, the use of the selectivity of the sandwich ELISA instead of the antibody selectivity for the characterization of an antibody contributed to this impression. In light of those findings, it is important to discriminate the antibody recognition from the immunoassay selectivity and to perform epitope mapping in developing nanobody-based sandwich ELISAs.

Matrix Effects. The detection of unknown samples is based on the premise that the analytes in the matrix may behave the same as the calibrators in the standard diluent. However, the matrix of real samples is actually different from the standard diluent. It may interfere with the binding between the antibody and antigen, thus generating a signal response of analytes that are different from that of the calibrators.[31] An efficient way to decrease the matrix effect is to dilute the biological sample with the standard diluent for matrix matching. The more diluted the sample, the closer the matrix of the samples matches that of the calibrators. As the matrix mainly interferes with the binding of the antibody and antigen in immunoassays, formats C and D were chosen to evaluate the matrix effects on sEH binding to pAb/nanobody and double nanobodies. Calibrators of mouse sEH in standard diluents and varying dilutions of liver cytosol samples from sEH KO mice at 1:100, 1:1000, and 1:10000 were prepared. Calibration curves of formats C and D against the above calibrators in the standard diluent and diluted samples were constructed and are illustrated in Figure 5. For simplicity, the overall recovery rate was calculated as the ratio of the slope of the calibration curve in diluted samples relative to that in standard diluents when the backgrounds were comparable. As shown in Figure 5a, the calculated overall recovery of format C was 105, 102, and 105% for the calibrators prepared at 1:100, 1:1000, and 1:10000 dilutions of the sample matrix, respectively. The corresponding overall

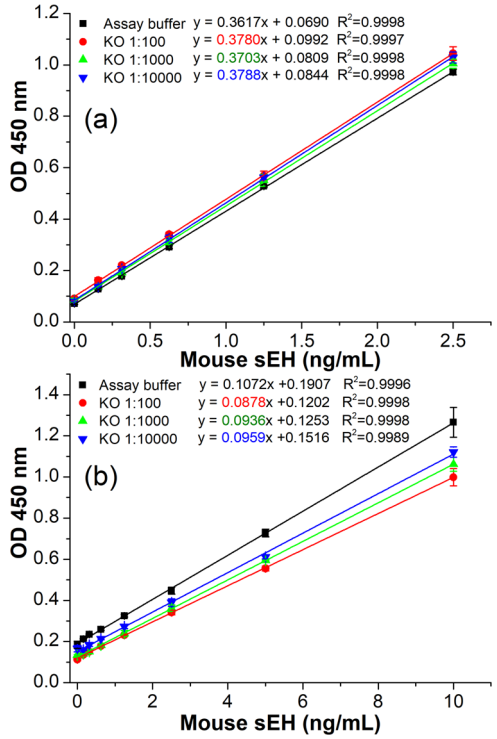

Figure 5. Comparison of signal responses of nanobody-based ELISAs in assay buffers and hepatic cytosol samples from KO mice at varying dilutions: (a) format C and (b) format D. Error bars indicate standard deviations (n = 3).

recovery of format D (see Figure 5b) was 82, 87, and 89%, respectively. It seems that format D was more susceptible to the matrix effect than format C. This was likely due to the potential interference resulting from the endogenous biotin in tissues,[32] which might displace some bound biotinylated capture nanobodies from the coated streptavidin. These data support the acceptance of nanobody-based ELISAs (format C and D) for mouse sEH analyses in biological samples.

Quantitation of Mouse sEH in Cancer Cells. Understanding the role of sEH in cancer development and therapy is the goal for biologists in the field.[33] However, the sEH expression in *in vitro* cell cultures is very low if present and is thus hard to track in cell models using classical western blot assays or regular immunoassays. In this work, the nanobody-based formats B and C with ultrahigh or high sensitivity were employed to measure the sEH level in eight murine cancer cell

https://dx.doi.org/10.1021/acs.analchem.0c01511
Anal. Chem. XXXX, XXX, XXX−XXX

Table 2. Summary of sEH Expression in Eight Strains of Mouse Cancer Cells Obtained with an ELISA (Format B) and Activity Level with the Radioactive Assay[a]

		ELISA (format B)					radioactive assay	
sample no.	cell name	sEH in diluted sample (pg/mL)	CV	±[b]	working dilution	sEH in neat sample (pg/mL)	activity	CV
1	Lewis lung cancer	2.1	5%	−	3.5	7.5	3.8	8%
2	T241 fibrosarcoma	1.2	13%	−	3.5	4.1	2.3	15%
3	B16F10 melanoma	3.0	5%	−	3.5	10.6	0.8	7%
4	4T1 breast adenocarcinoma	15.1	1%	+	3.5	52.9	2.9	9%
5	E0771 breast adenocarcinoma	120.6	2%	+	3.5	422.1	12.0	5%
6	MC38 colon adenocarcinima	3.3	8%	−	3.5	11.7	1.0	15%
7	CT26 colon adenocarcinoma	9.4	2%	+	3.5	33.0	26.8	4%
8	ID8 ovarian adenocarcinoma	2.4	2%	−	3.5	8.5	3.1	8%
9	E0771 breast adenocarcinoma	43.1	3%	+	10	430.8	10.3	5%
10	E0771 breast adenocarcinoma	40.1	1%	+	10	401.4	8.1	4%
11	CT26 colon adenocarcinoma	48.7	5%	+	1	48.7	26.5	3%
12	CT26 colon adenocarcinoma	46.6	0%	+	1	46.6	35.0	3%

[a]n = 3, if not otherwise specified. [b]Diluted samples with calculated values below the LOD (4 pg/mL) of the ELISA were recognized as negative. [c]Activity (pmol/(min·mL)) was measured using t-DPPO as the substrate.

lines. For better sensitivity, the incubation time for antigens and detection antibodies in formats C and B were extended from 1 to 2 h and 90 min, respectively; the working concentration of HRP-4C3 in format C was increased from 1:4000 to 1:2000. As demonstrated in Figure S5 and Table S2, format C demonstrated a sensitivity of 0.8226 OD·mL/ng and a LOD of 9.3 pg/mL. This enhanced ELISA only detected the sEH (0.340 and 0.335 ng/mL) without dilution of the cell extract derived from the E0771 breast adenocarcinoma (sample nos. 9 and 10). Meanwhile, format B gave a sensitivity of 5 OD·mL/ng and a LOD of 4.0 pg/mL. It could detect sEH expression at a 3.5-fold dilution of the 4T1 breast adenocarcinoma (sample no. 4), E0771 breast adenocarcinoma (sample no. 5), and CT26 colon adenocarcinoma (sample no. 7). Their calculated sEH levels in neat samples were 52.9, 422.1, and 33.0 pg/mL, respectively. Also, format B could confidently detect E0771 breast adenocarcinoma (sample nos. 9 and 10) at a 10-fold dilution and CT26 colon adenocarcinoma (sample nos. 11 and 12) at no dilution. The ultrahigh sensitivity of format B allows for a higher dilution and thus much smaller sample volumes than those of format C. This ultrasensitive format B could trace the sEH in samples that other formats were not able to detect. Its high sensitivity is pivotal for potential new discoveries in the field. In addition, good correlations between the sEH level and sEH activity were observed in our previous work.[18] However, again unexpectedly, the E0771 breast adenocarcinoma with the highest level of sEH (422.1 pg/mL) did not demonstrate the highest enzyme activity, and the CT26 colon adenocarcinoma with the highest sEH activity just showed relatively moderate sEH expression levels (33.0 pg/mL) in the first batch. This agreed with our pretest data before (data not shown). This discrepancy was reconfirmed repeatedly in the second batch of E0771 breast adenocarcinoma and CT26 colon adenocarcinoma cultured in duplicates. As shown in Table 2 (sample nos. 9−12) and Figure S5, the working dilutions gave strong signals that appeared in the central section of the calibration curve. The calculated sEH levels were 430.8 and 401.4 pg/mL in two E0771 breast adenocarcinoma samples and 48.7 and 46.6 pg/mL in two CT26 colon adenocarcinoma. Obviously, there is a dramatic difference in the sEH specific activity between E0771 breast adenocarcinoma and CT26 colon adenocarcinoma, as well as the other six kinds of cancer cells. It is unclear what the pathological significance is behind the difference. However, the ultrasensitive ELISA developed in this work provided a tool and clue for biologists in the field of cancer biology to investigate the unknown biological processes underlying this difference of sEH expression.

CONCLUSION

We developed four sandwich ELISA formats involving a combination of polyclonal antibodies and nanobodies for mouse sEH detection. It was found that the double antibodies worked as double filters and had a huge impact on both the sensitivity and selectivity of the sandwich immunoassays. The switch of anti-human sEH pAb to anti-mouse sEH pAb led to over a 100-fold increase in the sensitivity and a dramatic decrease of the LOD to a picogram per milliliter range in format B. Also, the double antibodies in all four formats generated better selectivities for mouse sEH recognition than the single antibody of pAb or nanobody alone assays. The four sandwich ELISAs favorably recognized the tissues of WT mice but not that of the sEH KO mice, whereas the pAb or nanobody alone assays showed significant cross-reactivity to the KO tissues. Finally, the ultrasensitive ELISA (format B) was used to successfully assess the level of sEH expression in eight strains of mouse cancer cells for the first time. Thus, the sandwich ELISAs developed in our work provided sensitive tools to trace the mouse sEH and a deep insight into the underlining dual filter effect of double antibodies in developing sandwich immunoassays.

ASSOCIATED CONTENT

Supporting Information

The Supporting Information is available free of charge at https://pubs.acs.org/doi/10.1021/acs.analchem.0c01511.

Nanobody sequences; selectivity of formats B, C, and D; selectivity of nanobodies and pAb; epitope mapping of nanobodies; photos and calibration curves for murine cancer cell analysis; sEH expression measured with format C (PDF)

https://dx.doi.org/10.1021/acs.analchem.0c01511
Anal. Chem. XXXX, XXX, XXX−XXX

AUTHOR INFORMATION

Corresponding Author

Bruce D. Hammock − *Department of Entomology and Nematology, University of California, Davis, Comprehensive Cancer Center, University of California, Davis, Davis, California 95616, United States;* orcid.org/0000-0003-1408-8317; Email: bdhammock@ucdavis.edu

Authors

Dongyang Li − *Department of Entomology and Nematology, University of California, Davis, Comprehensive Cancer Center, University of California, Davis, Davis, California 95616, United States;* orcid.org/0000-0002-5603-3608

Yongliang Cui − *Department of Entomology and Nematology, University of California, Davis, Comprehensive Cancer Center, University of California, Davis, Davis, California 95616, United States; Citrus Research Institute, Southwest University and National Citrus Engineering Research Center, Chongqing 400712, China*

Christophe Morisseau − *Department of Entomology and Nematology, University of California, Davis, Comprehensive Cancer Center, University of California, Davis, Davis, California 95616, United States*

Karen M. Wagner − *Department of Entomology and Nematology, University of California, Davis, Comprehensive Cancer Center, University of California, Davis, Davis, California 95616, United States*

Young Sik Cho − *Department of Entomology and Nematology, University of California, Davis, Comprehensive Cancer Center, University of California, Davis, Davis, California 95616, United States; Department of Pharmacy, Keimyung University, Daegu 42601, South Korea*

Complete contact information is available at: https://pubs.acs.org/10.1021/acs.analchem.0c01511

Author Contributions

D.L. and B.D.H. designed the research; D.L., Y.C., and C.M. performed the experiment; K.W. provided knockout and wild-type tissues; Y.S.C. cultivated the cancer cells; D.L., C.M., K.W., and B.D.H. analyzed the data and wrote the paper.

Notes

The authors declare no competing financial interest.

ACKNOWLEDGMENTS

The financial support from the National Institutes of Health (Superfund P42ES04699 and RIVER Award R35 ES030443-01) is acknowledged. D.L. is also grateful for the partial support from the National Natural Science Foundation of China (81402722) and the International Postdoctoral Exchange Fellowship (06/2014-06/2015) by the Office of China Postdoctoral Council. We also thank Dipak Panigrahy at Harvard Medical School for kindly providing the cancer cell lines and Jogen Atone at University of California, Davis, for performing the western blot experiments.

REFERENCES

(1) Morisseau, C.; Hammock, B. D. *Annu. Rev. Pharmacol. Toxicol.* **2013**, *53*, 37−58.

(2) Yao, L.; Cao, B.; Cheng, Q.; Cai, W.; Ye, C.; Liang, J.; Liu, W.; Tan, L.; Yan, M.; Li, B.; He, J.; Hwang, S. H.; Zhang, X.; Wang, C.; Ai, D.; Hammock, B. D.; Zhu, Y. *Am. J. Physiol. Gastrointest. Liver Physiol.* **2019**, *316*, G527−G538.

(3) Imig, J. D.; Hammock, B. D. *Nat. Rev. Drug Discovery* **2009**, *8*, 794−805.

(4) Morisseau, C.; Hammock, B. D. *Annu. Rev. Pharmacol. Toxicol.* **2005**, *45*, 311−333.

(5) Ren, Q.; Ma, M.; Yang, J.; Nonaka, R.; Yamaguchi, A.; Ishikawa, K.-i.; Kobayashi, K.; Murayama, S.; Hwang, S. H.; Saiki, S.; Akamatsu, W.; Hattori, N.; Hammock, B. D.; Hashimoto, K. *Proc. Natl. Acad. Sci. U. S. A.* **2018**, *115*, E5815−E5823.

(6) Borlongan, C. V. *Proc. Natl. Acad. Sci. U. S. A.* **2018**, *115*, 6322−6324.

(7) Morisseau, C.; Wecksler, A. T.; Deng, C.; Dong, H.; Yang, J.; Lee, K. S. S.; Kodani, S. D.; Hammock, B. D. *J. Lipid Res.* **2014**, *55*, 1131−1138.

(8) Morisseau, C.; Hammock, B. D. *Techniques for analysis of chemical biotransformation. Current Protocols in Toxicology*; Bus, J. S.; Costa, L. G.; Hodgson, E.; Lawrence, D. A.; Reed, D. J., Eds.; John Wiley & Sons, Inc.: NJ, 2007; pp 4.23.21−24.23.18.

(9) Ghosh, R.; Gilda, J. E.; Gomes, A. V. *Expert Rev. Proteomics* **2014**, *11*, 549−560.

(10) Huang, L.; Chen, J.; Yu, Z.; Tang, D. *Anal. Chem.* **2020**, *92*, 2809−2814.

(11) Xue, L.; Yang, Y.; Wu, S.; Huang, Y.; Li, J.; Xiang, Y.; Li, G. *Anal. Chem.* **2020**, *92*, 2972−2978.

(12) Zhan, Y.; Zeng, Y.; Li, L.; Guo, L.; Luo, F.; Qiu, B.; Huang, Y.; Lin, Z. *Anal. Chem.* **2020**, *92*, 1236−1244.

(13) Chen, Y.; Xianyu, Y.; Dong, M.; Zhang, J.; Zheng, W.; Qian, Z.; Jiang, X. *Anal. Chem.* **2018**, *90*, 6906−6912.

(14) Wang, K.; Vasylieva, N.; Wan, D.; Eads, D. A.; Yang, J.; Tretten, T.; Barnych, B.; Li, J.; Li, Q. X.; Gee, S. J.; Hammock, B. D.; Xu, T. *Anal. Chem.* **2019**, *91*, 1532−1540.

(15) Zhang, Y.-Q.; Xu, Z.-L.; Wang, F.; Cai, J.; Dong, J.-X.; Zhang, J.-R.; Si, R.; Wang, C.-L.; Wang, Y.; Shen, Y.-D.; Sun, Y.; Wang, H. *Anal. Chem.* **2018**, *90*, 12886−12892.

(16) Kim, H.-J.; McCoy, M. R.; Majkova, Z.; Dechant, J. E.; Gee, S. J.; Tabares-da Rosa, S.; González-Sapienza, G. G.; Hammock, B. D. *Anal. Chem.* **2012**, *84*, 1165−1171.

(17) Anderson, G. P.; Liu, J. L.; Hale, M. L.; Bernstein, R. D.; Moore, M.; Swain, M. D.; Goldman, E. R. *Anal. Chem.* **2008**, *80*, 9604−9611.

(18) Li, D.; Cui, Y.; Morisseau, C.; Gee, S. J.; Bever, C. S.; Liu, X.; Wu, J.; Hammock, B. D.; Ying, Y. *Anal. Chem.* **2017**, *89*, 6248−6256.

(19) Bruce, V. J.; McNaughton, B. R. *Anal. Chem.* **2017**, *89*, 3819−3823.

(20) Zhou, Q.; Li, G.; Chen, K.; Yang, H.; Yang, M.; Zhang, Y.; Wan, Y.; Shen, Y.; Zhang, Y. *Anal. Chem.* **2020**, *92*, 983−990.

(21) Fan, K.; Jiang, B.; Guan, Z.; He, J.; Yang, D.; Xie, N.; Nie, G.; Xie, C.; Yan, X. *Anal. Chem.* **2018**, *90*, 5671−5677.

(22) Morales-Yánez, F.; Trashin, S.; Hermy, M.; Sariego, I.; Polman, K.; Muyldermans, S.; De Wael, K. *Anal. Chem.* **2019**, *91*, 11582−11588.

(23) Pírez-Schirmer, M.; Brena, B. M.; González-Sapienza, G. *Anal. Chem.* **2019**, *91*, 9925−9931.

(24) Cui, Y.; Li, D.; Morisseau, C.; Dong, J.-X.; Yang, J.; Wan, D.; Rossotti, M.; Gee, S.; González-Sapienza, G.; Hammock, B. *Anal. Bioanal. Chem.* **2015**, *407*, 7275−7283.

(25) Belanger, L.; Sylvestre, C.; Dufour, D. *Clin. Chim. Acta* **1973**, *48*, 15−18.

(26) Yamada, T.; Morisseau, C.; Maxwell, J. E.; Argiriadi, M. A.; Christianson, D. W.; Hammock, B. D. *J. Biol. Chem.* **2000**, *275*, 23082−23088.

(27) Pinot, F.; Grant, D. F.; Beetham, J. K.; Parker, A. G.; Borhan, B.; Landt, S.; Jones, A. D.; Hammock, B. D. *J. Biol. Chem.* **1995**, *270*, 7968−7974.

(28) Li, D.; Morisseau, C.; McReynolds, C. B.; Duflot, T.; Bellien, J.; Nagra, R. M.; Taha, A. Y.; Hammock, B. D. *Anal. Chem.* **2020**, *92*, 7334−7342.

(29) Aeonian Biotech. *What is the difference between antibody's specificity and its selectivity?* https://aeonianbiotech.com/what-is-the-

https://dx.doi.org/10.1021/acs.analchem.0c01511
Anal. Chem. XXXX, XXX, XXX−XXX

difference-between-antibodys-specificity-and-its-selectivity/ (accessed Mar 31, 2020).
(30) Hudson, L.; Liu, J.; Nath, A.; Jones, M.; Raghavan, R.; Narayan, O.; Male, D.; Everall, I. *J. NeuroVirol.* **2000**, *6*, 145−155.
(31) Tate, J.; Ward, G. *Clin. Biochem. Rev.* **2004**, *25*, 105−120.
(32) Trambas, C.; Lu, Z.; Yen, T.; Sikaris, K. *Ann. Clin. Biochem.* **2018**, *55*, 205−215.
(33) Zhang, J.; Sanidad, K. Z.; Zhang, G. *Oncoscience* **2019**, *6*, 371−375.

https://dx.doi.org/10.1021/acs.analchem.0c01511
Anal. Chem. XXXX, XXX, XXX−XXX